Elastic cross sections for electron scattering from GeF4: Predominance of atomic-F in the high-energy collision dynamics

H. Kato, A. Suga, M. Hoshino, F. Blanco, G. García et al.

Citation: J. Chem. Phys. **136**, 134313 (2012); doi: 10.1063/1.3699040
View online: http://dx.doi.org/10.1063/1.3699040
View Table of Contents: http://jcp.aip.org/resource/1/JCPSA6/v136/i13
Published by the American Institute of Physics.

Elastic cross sections for electron scattering from GeF_4: Predominance of atomic-F in the high-energy collision dynamics

H. Kato,[1] A. Suga,[1] M. Hoshino,[1] F. Blanco,[2] G. García,[3] P. Limão-Vieira,[1,4]
M. J. Brunger,[5,6,a)] and H. Tanaka[1]
[1]*Department of Physics, Sophia University, Tokyo 102-8554, Japan*
[2]*Departamento de Fisica Atomica, Molecular y Nuclear, Facultad de Ciencias Fisicas, Universidad Complutense de Madrid, E-28040 Madrid, Spain*
[3]*Instituto de Fisica Fundamental, Consejo Superior de Investigaciones Cientficas, 28006 Madrid, Spain*
[4]*CEFITEC, Departamento de Física, Faculdade de Ciéncias e Tecnologia, Universidade Nova de Lisboa, 2829-516 Caparica, Portugal*
[5]*ARC Centre for Antimatter-Matter Studies, Flinders University, GPO Box 2100, Adelaide, SA 5001, Australia*
[6]*Institute of Mathematical Sciences, University of Malaya, Kuala Lumpur 50603, Malaysia*

(Received 9 February 2012; accepted 14 March 2012; published online 4 April 2012)

We report absolute differential cross sections (DCSs) for elastic electron scattering from GeF_4. The incident electron energy range was 3–200 eV, while the scattered electron angular range was typically 15°–150°. In addition, corresponding independent atom model (IAM) calculations, within the screened additivity rule (SCAR) formulation, were also performed. Those results, particularly for electron energies above about 10 eV, were found to be in good quantitative agreement with the present experimental data. Furthermore, we compare our GeF_4 elastic DCSs to similar data for scattering from CF_4 and SiF_4. All these three species possess T_d symmetry, and at each specific energy considered above about 50 eV their DCSs are observed to be almost identical. These indistinguishable features suggest that high-energy elastic scattering from these targets is virtually dominated by the atomic-F species of the molecules. Finally, estimates for the measured GeF_4 elastic integral cross sections are derived and compared to our IAM-SCAR computations and with independent total cross section values. © *2012 American Institute of Physics*. [http://dx.doi.org/10.1063/1.3699040]

I. INTRODUCTION

Despite the importance of GeF_4 in the chemistry of some low-temperature plasmas, in particular when associated with the manufacturing of semiconductors, we are not aware of any previous experimental data for elastic electron scattering differential cross sections (DCSs) or integral cross sections (ICSs) from this species. Indeed, for the elastic channel, we only know of results from a theoretical calculation[1] at the DCS and ICS level, although we note only tabulated values of their ICS are provided. That calculation was conducted at intermediate and high impact energies, using the independent atom model (IAM) approach with a model static-polarisation-exchange potential.[1] Results for excitation of other scattering channels are fragmentary but include dissociative attachment,[2] vacuum ultraviolet fluorescence,[3] an electron energy loss spectroscopy (EELS) investigation into discrete inelastic channels by Kuroki *et al.*,[4] an electron impact ionisation study from Mason and Tuckett,[5] and finally total cross sections (TCSs), from 0.5–250 eV impact energies, using a linear transmission approach, due to Szmytkowski *et al.*[6] Hence, one rationale for the present work is to improve, at least in part, this deficiency in the literature in terms of our knowledge and understanding for electron–GeF_4 scattering.

Since the very foundations of atomic and molecular collision experiments, scientists[7,8] have been interested in studying trends (similarities and differences) in results from electron scattering from related series of atoms and molecules. Such series might include the noble gases, simple organic molecule homologous series such as C_nH_{2n+2} (for $n \geq 1$),[9–12] the halomethane series CH_3X (X=F, Cl, Br and I; Ref. 13), and finally the series XH_4, where X=C, Si, and Ge.[14] For example, in their work on elastic electron scattering from the halomethane series CH_3F, CH_3Cl, CH_3Br, and CH_3I, Kato *et al.*[13] found very similar DCS behaviour at 50 eV, 100 eV, and 200 eV when they compared those results to the corresponding elastic cross sections in Ne, Ar, Kr, and Xe. Similarly, when the high-energy elastic DCS of Ne, Ar, and Kr were compared to those of their isoelectronic molecular counterparts CH_4, SiH_4, and GeH_4,[14] very good accord was again observed. This led these authors[13,14] to propose that in high-energy (≥50 eV) electron scattering processes, "atomic-like" effects prevail. Recently, Limão-Vieira *et al.*[15] have also shown this behaviour by comparing the CCl_4 elastic cross sections to results on CH_3Cl and atomic chlorine at higher input energies. Further evidence in support of this notion of "atomic-like" effects being important in high-energy elastic scattering, can be seen in the excellent agreement between the IAM-SCAR results from the Madrid group and available experimental data, even for quite complicated molecules.[13,14,16] As a consequence, here we further investigate this idea by comparing elastic DCS results for the molecular series XF_4,

a)Electronic mail: Michael.Brunger@flinders.edu.au.

TABLE I. Present experimental differential cross sections ($\times 10^{-16}$ cm^2/sr) for elastic electron scattering from GeF_4. Also listed at the foot of the table are the elastic ICS ($\times 10^{-16}$ cm^2) and MTCS ($\times 10^{-16}$ cm^2) that we derived from our DCS using a modified phase shift analysis approach or the results from our IAM–SCAR computations.

Angle	Impact energy (eV)								
(deg)	3.0	5.0	7.0	10	20	30	50	100	200
15	4.1261	9.5939	...	...	...	...	...	...	3.6411
20	4.3487	8.4618	8.0916	...	...	...	8.8410	2.5726	3.1094
30	3.0024	5.5711	6.7675	7.6649	8.5004	3.8973	1.5644	1.7717	1.0728
40	2.2840	4.1660	4.9376	5.1203	3.2129	1.2068	1.4521	0.6933	0.6661
50	1.8241	3.4385	3.4140	3.1974	1.8803	1.5942	1.1480	0.3770	0.3519
60	1.7317	2.6552	2.1715	2.2074	1.8425	1.6924	0.5833	0.3898	0.2180
70	1.8330	2.0912	1.7075	1.5728	1.6234	1.0135	0.4026	0.2265	0.0795
80	1.9465	1.8694	1.4049	1.2847	0.9709	0.5811	0.3202	0.1129	0.0746
90	2.0273	1.5953	1.1200	1.1121	0.5836	0.5953	0.1788	0.0954	0.0951
100	2.0537	1.3506	0.8424	0.8447	0.5025	0.5251	0.1217	0.1688	0.1133
110	1.9623	1.0214	0.6474	0.6389	0.6280	0.4806	0.1970	0.2276	0.1001
120	1.9697	0.6986	0.5598	0.7445	0.8165	0.5583	0.3105	0.2948	0.0958
130	1.8221	0.6038	0.7698	1.0710	0.9492	0.8219	0.4667	0.3326	0.0829
140	...	...	...	...	...	...	0.7076	0.4670	0.1173
150	...	...	...	...	...	...	0.8414	0.5312	0.1528
ICS	26.713	29.758	28.571	30.274	30.035	24.921	14.843	11.32	6.96
MTCS	25.070	19.634	16.639	16.661	14.691	12.674	6.488	5.73	4.07

where X=C, Si, and Ge. Note that in doing so, the CF_4 elastic DCS of Boesten *et al.*[17] are employed, while those for SiF_4 are taken from the unpublished work of Kato *et al.*[18]

In Sec. II, we give details of our experimental apparatus and measurement techniques, while in Sec. III a brief description of the present IAM-SCAR computations is provided. Thereafter, in Sec. IV, our results and a discussion of those results are presented, before some conclusions from this investigation are drawn.

II. EXPERIMENTAL DETAILS

The present measurements were carried out in two crossed electron molecular-beam spectrometers. The original spectrometer has been described in detail many times (see, e.g., Boesten *et al.*[10]), while a description of the newer apparatus is given in Kato *et al.*[13] Both these systems contain common elements, including hemispherical monochromators and analysers, a series of electron-lens systems to transport and focus the electron beam, as controlled in both cases by computer-driven voltages, and differential pumping of the electron optics.

In this study, the original spectrometer operated at fixed incident electron energies between 3–30 eV and over the scattered electron angular range -20 to $+130^\circ$. The energy resolution in this set-up was typically maintained at $\sim$35 meV (FWHM), which should be sufficient to exclude any contributions from the lower vibrational modes of GeF_4 to the measured elastic signal. This is no moot point here, as in particular at 3 eV there is a Ramsauer-Townsend minimum in the TCS.[6] Thus, if the situation in CF_4 (Ref. 17) can be taken as a guide, the vibrational excitation cross sections at this energy may make a substantial contribution to the TCS. As a consequence, it is important we eliminate their possible contribution to our elastic scattering signal, in order to avoid a systematic error in the elastic GeF_4 DCSs we report. The newer spectrometer[13] was operated at either 50, 100 or 200 eV impact energy, with a scattered electron angular range of $\theta = -20$ to $+150^\circ$. In this case, the energy resolution was relaxed to $\sim$90 meV (FWHM), as at these relatively high energies the vibrational excitation cross sections are expected to be so small that any contribution they might make to the elastic signal can be safely ignored. For both these spectrometers, the impact energy scale was calibrated by either reference to the well-known ^{2}S resonance in He at 19.367 eV, or the first peak in the $\nu = 0 - 1$ excitation function in N_2 at $\sim$1.97 eV (Ref. 19) or to both these features as an additional cross check. The angular resolution of the present spectrometers was 1.5° (FWHM), with the true zero scattering angle being determined in each case by the symmetry of the He 2^1P inelastic intensity about the nominal 0° point. The molecular beam was produced effusively in each spectrometer through a simple tube of length 5 mm and diameter 0.3 mm, kept at slightly elevated temperatures (50–70°C) throughout the measurements in order to avoid any contamination of GeF_4 on the nozzle surface. Note that our GeF_4 sample was sourced from the Takachiho Chemical Company with a stated purity better than 99.9%.

The observed elastic scattering intensities were converted into absolute cross sections (see Table I), at each incident electron energy and scattered electron angle (θ), by using the now standard relative flow technique.[12,20] In the present application of the relative flow technique, He was employed as the reference gas with its cross sections taken from the extensive compilation of Boesten and Tanaka.[21] This implies adjustment of the relative gas (GeF_4, He) pressures to ensure their Knudsen numbers are approximately equal, thereby engineering that both their gas beam profiles remain similar. In this work, the driving pressures behind the nozzle were about 0.2 Torr for GeF_4 and 2 Torr for He. There have been persistent reports in the literature in respect to non-linearities in the

measured normalised flow rates versus driving pressures,[12,22,23] even for simple gases such as N_2. However, no such non-linear behaviour was observed in the present investigation. In all cases, i.e., at each impact energy and θ and for whichever spectrometer was used, great care was also exercised to ensure the background contribution was correctly identified and subtracted from the measured elastic scattering intensity prior to the normalisation. Finally, note that both spectrometers are operated in parallel thus reducing the time needed to undertake the experimental component of this study.

The present elastic DCSs were extrapolated to 0° and 180°, using either the corresponding shapes of our IAM–SCAR computations (see Sec. III) as a guide or a modified phase shift analysis (MPSA), before being integrated at each energy using Eqs. (1) and (2) below, to determine the ICSs and momentum transfer cross sections (MTCS) via

$$\mathrm{ICS} = 2\pi \int_0^{\pi} \mathrm{DCS}(\theta) \sin\theta \mathrm{d}\theta, \tag{1}$$

$$\mathrm{MTCS} = 2\pi \int_0^{\pi} \mathrm{DCS}(\theta)(1 - \cos\theta) \sin\theta \mathrm{d}\theta. \tag{2}$$

These derived ICS and MTCS are tabulated at the foot of Table I. Note that we might expect those integrals to be fairly insensitive to the details of the extrapolation (for $\theta < 15°$ and $\theta > 130°$ or 150°, depending on the spectrometer employed in DCS measurements), due to GeF_4 being a non-polar molecule and the presence of $\sin\theta$ in the integrands of Eqs. (1) and (2). Nonetheless at energies less than 20 eV, normally where the measured and calculated angular distributions are sometimes in not so good agreement (see Fig. 1), we also employed a MPSA, e.g., Ref. 24 that uses a Thompson correction for the higher-order partial waves[25] and a value for the dipole polarisability of GeF_4 of $\alpha = 6.5 \times 10^{-24}$ cm^3.[26] The results of this analysis are shown in Fig. 1, where we see good quality fits are found at each relevant energy. In most cases, the derived elastic ICS and MTCS were consistent with one another, irrespective of the approach used to perform the extrapolation, with the major exception being the result at 3 eV. We shall return to this point later in our discussion in Sec. IV. Note, however, that all the ICS and MTCS given in the foot of Table I represent our best estimates for those cross sections.

Finally, we note that the overall uncertainties on the measured GeF_4 elastic DCSs lie in the range 15% –20% while those for the ICS are ∼25% and for the MTCS they are ∼30% –35%. The largest component of the error on the elastic DCS is due to the uncertainty in the cross sections of the reference gas (∼10%),[21] while the additional uncertainty in the values of the ICS and MTCS is due to errors associated with the extrapolation process.

III. NUMERICAL CONSIDERATIONS

The first subjects of the present calculations are the atoms constituting GeF_4, namely, Ge and F. We represent each atomic target by an interacting complex potential (i.e., the optical potential), whose real part accounts for the elastic scattering of the incident electrons, while the imaginary part represents the inelastic processes that are considered as "absorption" from the incident beam. To construct this complex potential for each atom, the real part of the potential is represented by the sum of three terms: (i) a static term derived from a Hartree-Fock calculation of the atomic charge distribution,[27] (ii) an exchange term to account for the indistinguishability of the incident and target electrons,[28] and (iii) a polarisation term[29] for the long-range interactions which depend on the target dipole polarisability.[26] The imaginary part, following the procedure of Staszewska *et al.*,[30] then treats inelastic scattering as electron–electron collisions. However, we initially found some major discrepancies in the available scattering data, which were subsequently corrected when a physical formulation of the absorption potential[31] was introduced. Further improvements to the original formulation,[30] such as the inclusion of screening effects, local velocity corrections, and in the description of the electrons' indistinguishability,[32] finally led to a model that provides a good approximation of electron–atom scattering over a broad energy range. An excellent example of this was for elastic electron–atomic iodine (I) (Ref. 33) scattering, where the optical potential results compared very favourably with those from an independent highly sophisticated Dirac-B-spline R-matrix computation.

To calculate the cross sections for electron scattering from GeF_4, we follow the IAM by applying what is commonly known as the AR. In this approach, the molecular scattering amplitude is derived from the sum of all the relevant atomic amplitudes, including the phase coefficients, which lead to the molecular DCSs for the molecule in question. Integral cross sections can then be determined by integrating those DCSs, with the sum of the elastic ICS and the absorption ICS (for all inelastic processes except rotations and vibrations) then giving the TCSs. Alternatively, the ICSs for GeF_4 can also be derived from the relevant atomic ICSs in conjunction with the optical theorem.[32] Unfortunately, in its original form, we found an inherent contradiction between the ICSs derived from those two approaches, which suggested that the optical theorem was being violated.[34] This conundrum, however, has been resolved[34] by employing a normalisation procedure during the computation of the DCSs, so that the ICSs derived from the two approaches are now entirely consistent.[34] A limitation of the AR is that no molecular structure is considered, so that it is really only applicable when the incident electrons are so fast that they effectively see the target molecule as a sum of individual atoms (typically above ∼100 eV). To reduce this limitation, García and Blanco[35,36] introduced the SCAR method, which considers the geometry of a relevant molecule (atomic positions and bond lengths) by using some screening coefficients. With this correction, the range of validity of the IAM-SCAR approach might be extended to incident electron energies of 50 eV or a little lower. Indeed, it is the elastic DCS and ICS results from the application of the IAM–SCAR method to GeF_4 that we report on here.

IV. RESULTS AND DISCUSSION

In Table I and Fig. 1, we present the current elastic differential cross sections for electron scattering from GeF_4. Also

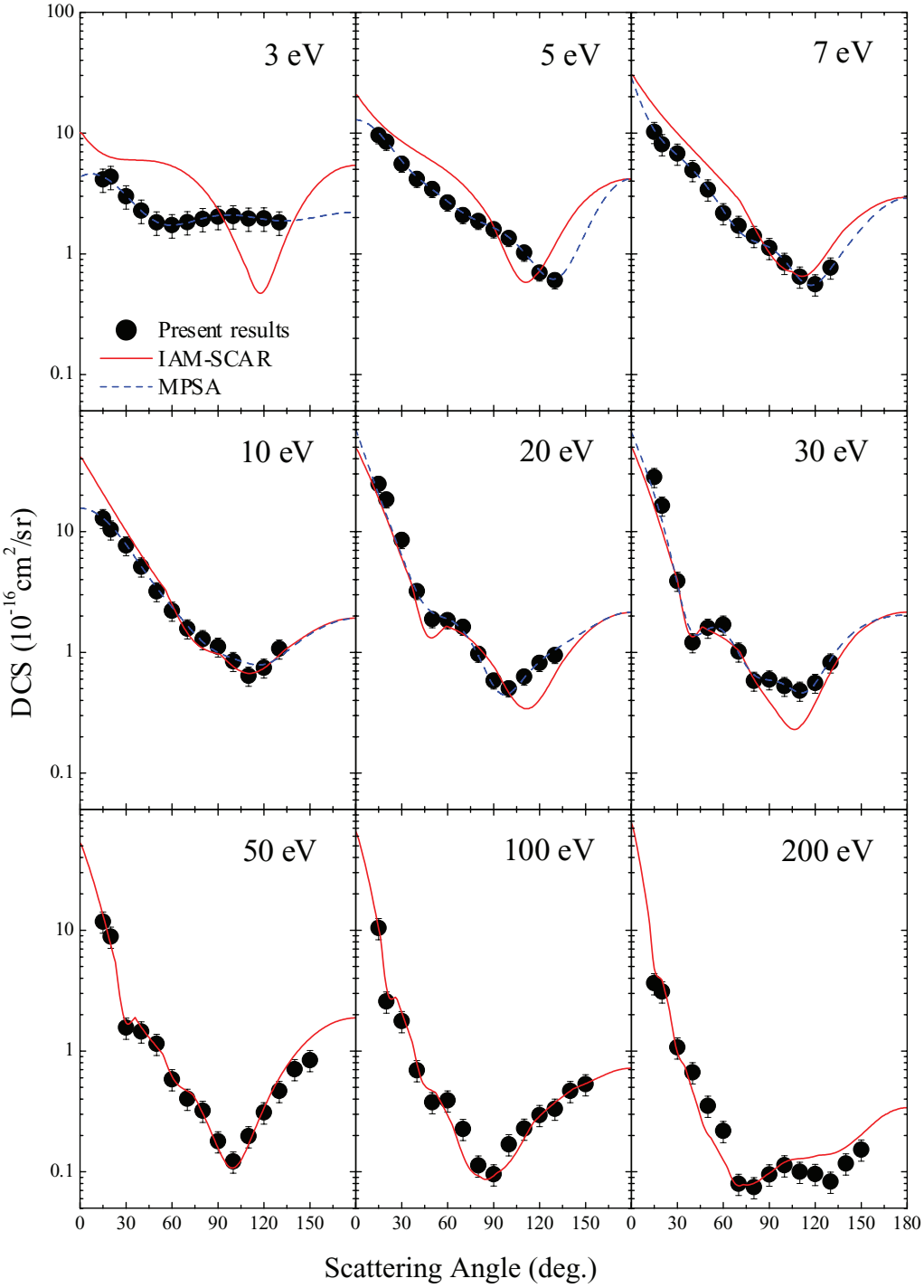

FIG. 1. Present measured (•) differential cross sections ($\times 10^{-16}$ cm^2/sr) for elastic electron scattering from GeF_4. Also shown are the results from our IAM–SCAR computations (—) and, where appropriate, our modified phase shift analysis, MPSA, (- - - -).

plotted in Fig. 1 are the corresponding results from our IAM–SCAR computations, and for energies between 3 and 30 eV the results from our modified phase shift analysis fits to the present DCSs. The first point we notice from the montage of cross sections that we show in Fig. 1 is just how radically the angular distributions of the various DCSs change as you increase the impact energy from 3 eV to 200 eV. These changes intimately reflect the differences between the dominant physical processes (e.g., exchange versus direct scattering), and their interplay, affecting the scattering dynamics at the various kinematical conditions of our study. At the higher impact energies of this investigation we would expect direct scattering to dominate the interaction. As GeF_4 possesses no permanent dipole moment, we anticipate that the strong forward peaking we observe in the magnitude of the DCSs at those higher energies, which progressively increases as one goes from 3 eV to 200 eV impact energies, reflects (at least in part) the relatively large value of the dipole polarisability for GeF_4. While it is clear from Fig. 1 that this peaking in the angular distributions diminishes as you go to lower energies,

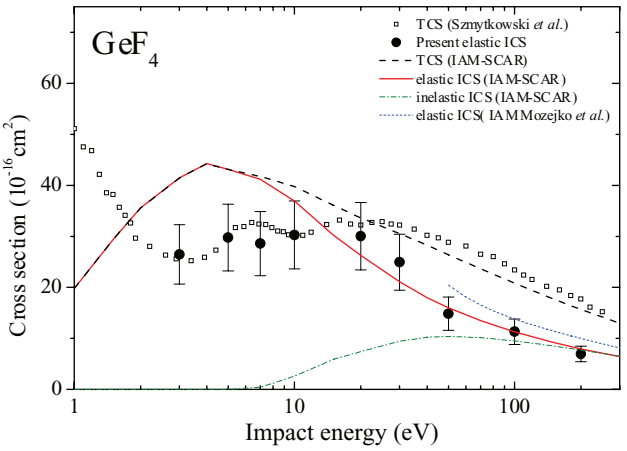

FIG. 2. Present measured (•) elastic integral cross sections ($\times 10^{-16}$ cm^2) for electron scattering from GeF_4. Also shown are the current elastic (—), total inelastic (– · – ·), and total (– – –) cross section results from our IAM–SCAR calculations. An earlier TCS measurement (□) from Szmytkowski *et al.*[6] and elastic ICS calculation (IAM) from Możejko *et al.*[1] (- - - - -) are also shown.

it never entirely disappears. This suggests to us that the dipole polarisability of the target molecule plays an important role in the direct scattering process, albeit diminished at the lower energies, throughout the kinematical range of the present measurements. Indeed even at 3 eV, which is at the nadir of the Ramsauer-Townsend minimum,[6] we see evidence for its contribution to the collisional dynamics. The angular distribution of the 3 eV DCS is very different to those at the other energies, being almost isotropic for scattering angles greater than about 60°. We ascribe this behaviour to the effects of the Ramsauer-Townsend minimum, where one of the main scattering eigenphases is expected to tend to 0 radian. Another interesting feature of the angular distributions in Fig. 1 is that the main angular minimum in the DCS moves from an angle of ∼120° at 5 eV (no minimum is observed experimentally at 3 eV) to an angle of ∼75° at 200 eV. We note that this same behaviour is semi-quantitatively reproduced by our IAM–SCAR calculations. The total cross section experiments of Szmytkowski *et al.*[6] (see also Fig. 2) predict a shape resonance with a peak centred at about 6.5–7 eV impact energy. No discernible evidence for this resonance can be gleaned from our 7 eV elastic DCS, suggesting perhaps that the main decay channel for this shape resonance might be into one or more of the relevant vibrational excitation modes of GeF_4.

Perhaps the most striking feature of Fig. 1, is just how quantitatively well the IAM–SCAR calculation reproduces the measured DCSs at energies greater than and including 10 eV. While there does remain differences in some details between experiment and theory in the 10–200 eV energy range, their overall level of accord is really quite remarkable. Indeed even at 7 eV, the qualitative (shape) agreement between them is still fairly good. While we had anticipated, on the basis of past experience,[13] finding a reasonable correspondence between the data and theory for energies $E \geq 50$ eV, the lower energy agreement was a surprise. In effect, for GeF_4, this observation is suggesting that the computationally "cheap" (compared to fully *ab initio* electron–molecule theoretical approaches) SCAR approach, is providing here a reasonable description for the molecular nature of this species down to energies as low as ∼10 eV.

We now extrapolate and integrate the DCS of Fig. 1, in the manner described earlier, to generate elastic ICS and MTCS. Those cross sections can be found at the foot of Table I, while the present elastic integral cross sections are also plotted, along with our corresponding IAM–SCAR results, in Fig. 2. In addition, in Fig. 2, we also plot the sum of all the integral inelastic (electronic state excitation and ionisation mainly but not accounting for rotations and vibrational excitation) IAM–SCAR cross sections, the IAM–SCAR total cross section, and the measured TCS from Szmytkowski *et al.*[6] Given our previous discussion at the DCS level, it is not surprising to find that our experimental and theoretical elastic ICS are in very good agreement with one another, to within the experimental uncertainties, for energies between 10 and 200 eV. At lower energies, however, the current calculation overestimates somewhat the magnitude of the measured elastic ICS. Nonetheless, our lower energy ICSs track well the result of the independent TCS data,[6] with the possible exception of the result at 7 eV. This energy coincides with the peak in the shape resonance (see Fig. 2), so that if our previous assertion as to this resonance decaying preferentially into the vibrational channels was correct, the relatively poorer accord at 7 eV might simply reflect that our elastic ICS does not account for vibrational excitation whereas the TCS does. Note that as vibrational cross sections are usually only significant if resonantly enhanced, this argument does not affect the good accord between our elastic ICS and the TCS (Ref. 6) that we find at 3 eV, 5 eV, and 10 eV, i.e., away from the shape resonance, as vibrational excitation cross sections at those energies can be reasonably anticipated to be small.[12] For energies $E \geq 30$ eV, the present elastic ICS are seen (Fig. 2) to be significantly smaller in magnitude than the TCS results. However, this can simply be understood as being due to our elastic ICS not accounting for the effects of discrete electronic state excitation and in particular ionisation. Indeed, if we were to add our calculated IAM–SCAR result, for the sum over all the inelastic cross sections, to our measured elastic ICS, then the resultant cross section would be in excellent agreement with the independent TCS measurement for all $E \geq 30$ eV. With respect to the efficacy of the data in Fig. 2 for low-temperature plasma modelling, for a plasma reactor containing GeF_4, it appears that the IAM–SCAR elastic ICS results could be safely employed for $E \geq 20$ eV, whereupon at the lower energies ($E < 20$ eV) the measured data should be "spliced" onto those IAM–SCAR results. Finally, we have included the MTCS results in the foot of Table I, even though we do not discuss them here. This is because MTCS are very useful data for kinetic transport modellers who seek to simulate the behaviour of electrons as they drift and diffuse, under the influence of an applied electric field or crossed electric and magnetic fields, through the gas in question.

In Fig. 3, we now compare the elastic DCS results from our group, for electron scattering from CF_4,[17] SiF_4,[18] and the present GeF_4 work. Note that for CF_4 at 200 eV, we have also used the independent results from Sakae *et al.*[37] in order to complete this comparison. While CF_4, SiF_4, and GeF_4 all have tetrahedral (T_d) symmetry and none of them possess

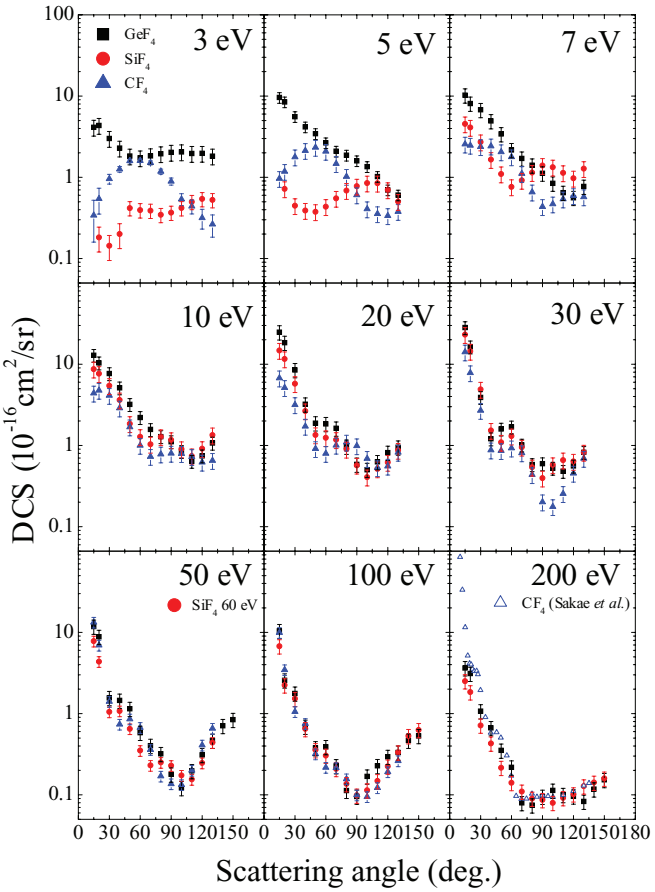

FIG. 3. Elastic differential cross sections ($\times 10^{-16}$ cm^2/sr) for electron scattering from GeF_4 (■) present data, SiF_4 (red ●),[18] and CF_4 (blue ▲; Ref. 17). Errors plotted are the overall errors on the DCSs and are at the one standard deviation level.

a permanent dipole moment, they are in fact each a unique species. This, for example, can be evidenced by their different dipole polarisabilities[26] ($\alpha = 3.87 \times 10^{-24}$ cm^3 for CF_4; $\alpha = 5.45 \times 10^{-24}$ cm^3 for SiF_4; $\alpha = 6.50 \times 10^{-24}$ cm^3 for GeF_4) and the fact that the C–F bond length in CF_4 (1.35 Å; Ref. 38) is slightly shorter than the Si–F bond length in SiF_4 (1.60 Å; Ref. 38) which in turn is shorter compared to the Ge–F bond length in GeF_4 (1.68 Å).[38] As a consequence we might reasonably, *a priori*, expect the collisional dynamics for elastic electron scattering from each of these molecules, at a given impact energy, to be unique so that their corresponding differential cross sections will be rather different. Indeed the case for this is further strengthened when one considers that the energies at which the incident electrons might attach to these respective species, possibly leading to resonant enhancement of their cross sections, are also likely to be different in each case. Our expectation for differences in their cross sections is precisely what we find in Fig. 3, for impact energies of 3 eV, 5 eV, and 7 eV. Here, the angular distributions, at each energy and for each species, are very different, although a definitive explanation for what factors cause those differences awaits applications of *ab initio* level scattering theory. Somewhat surprisingly, for energies between 10 and 30 eV, the angular distributions for each of these species now start to become very similar, the exception being for CF_4 at 30 eV and for scattering angles between 90°and 120°, with major differences really only manifesting themselves in terms of the absolute magnitudes of their DCSs. For instance, in this energy range, it is apparent that the CF_4 differential cross sections tend to be uniformly lower in magnitude (at a given energy) compared to those of SiF_4 and GeF_4 (see Fig. 3). However, the most startling feature in Fig. 3 is that for energies $E \geq 50$ eV, and to within the experimental uncertainties on each of the DCS data, the cross sections at a given energy and for each species are largely identical. This was not what we had expected, and we can only rationalise it by suggesting that at these higher impact energies, the incident electron is effectively only "seeing" the charge cloud produced by the four fluorine atoms. Put another way, the higher energy DCS data in Fig. 3 appear to be indicating that the centrally bonded carbon, silicon, and germanium atoms are largely behaving as spectators in the collision process at those energies. If correct then we have another example (see, e.g., Ref. 13) for where "atomic-like" effects persist in each of these species (CF_4, SiF_4, and GeF_4), where in reality we should essentially be dealing with scattering from molecular species. Note, investigating whether such behaviour also extended to the series CCl_4, $SiCl_4$, and $GeCl_4$ would be interesting, and potentially might provide further evidence in support of this notion.

V. CONCLUSIONS

We have reported measurements of absolute elastic differential cross sections for electron scattering from GeF_4. Corresponding theoretical cross sections, calculated within the IAM–SCAR approach, were also presented and found to be in very good agreement with the experimental data for energies greater than about 20 eV. This indicated that the present SCAR approach, which incorporates the effects of molecular structure, has been rather successful in extending the validity of the standard IAM paradigm to energies below 50 eV. Integral elastic and momentum transfer cross sections, as derived from the measured DCSs, were also determined as a part of this study. The present experimental elastic ICS were also, at energies above 10 eV, found to be in good accord with the IAM–SCAR results, as you would expect on the basis of the comparison at the DCS level. These ICSs were also found to be largely consistent with independent TCS measurements.[6] Finally, by comparing the present GeF_4 DCSs with those from CF_4 (Ref. 17) and SiF_4,[18] at a given energy, we observed that at energies above (and including) 50 eV they were all largely identical. In other words, irrespective of the nature of the centrally bonded atom (C or Ge or Si) the measured cross sections had the same magnitude. This led us to conclude that in these species, at the higher impact energies, the scattering dynamics were largely dominated by the atomic-F species that surround the central atom. This, in turn, provided further support for the notion of "atomic-like" effects persisting in what are fundamentally electron–molecule scattering systems.

ACKNOWLEDGMENTS

This work was conducted under the support of the Japanese Ministry of Education, Sport, Culture and Technology and the Australian Research Council through its Centres of Excellence program. This work also forms part of the EU/ESF COST Action MP1002 "Nanoscale Insights into Ion Beam Cancer Therapy (Nano-IBCT)". P.L.-V. acknowledges his Visiting Professor position at Sophia University, Tokyo, Japan while M.J.B. thanks the Japan Society for the Promotion of Science, for the award of a Short-term Fellowship that enabled him to visit Sophia University. Finally, P.L.-V., G.G., and F.B. acknowledge partial financial support of the Spanish Ministerio de Ciencia e Innovacíon (Project No. FIS2009–10245) and the Portuguese-Spanish joint collaboration through the bilateral Project No. HP2006-0042.

[1]P. Możejko, B. Żywicka-Możejko, and C. Szmytkowski, Nucl. Instrum. Methods B **196**, 245 (2002).
[2]P. W. Harland, S. Cradock, and J. C.J. Thynne, Int. J. Mass Spectrom. Ion Phys. **10**, 169 (1972).
[3]K. J. Boyle, D. P. Seccombe, R. P. Tuckett, H. Baumgärtel, and H. W. Jochims, Chem. Phys. Lett **294**, 507 (1998).
[4]K. Kuroki, D. Spence, and M. A. Dillon, J. Electron Spectrosc. Relat. Phenom. **70**, 151 (1994).
[5]S. M. Mason and R. P. Tuckett, Mol. Phys. **62**, 979 (1987).
[6]C. Szmytkowski, P. Możejko, and G. Kasperski, J. Phys. B **31**, 3917 (1998).
[7]F. L. Arnot, Proc. R. Soc. London A **144**, 360 (1934).
[8]S. Hill and A. H. Woodcock, Proc. R. Soc. London A **155**, 331 (1936).
[9]L. Boesten and H. Tanaka, J. Phys. B **24**, 821 (1991).
[10]L. Boesten, H. Tanaka, M. Kubo, H. Sato, M. Kimura, M. A. Dillon, and D. Spence, J. Phys. B **23**, 1905 (1990).
[11]L. Boesten, M. A. Dillon, H. Tanaka, M. Kimura, and H. Sato, J. Phys. B **27**, 1845 (1994).
[12]M. J. Brunger and S. J. Buckman, Phys. Rep. **357**, 215 (2002).
[13]H. Kato, T. Asahina, H. Masui, M. Hoshino, H. Tanaka, H. Cho, O. Ingólfsson, F. Blanco, G. Garcia, S. J. Buckman, and M. J. Brunger, J. Chem. Phys. **132**, 074309 (2010).
[14]M. A. Dillon, L. Boesten, H. Tanaka, M. Kimura, and H. Sato, J. Phys. B **26**, 3147 (1993).
[15]P. Limão-Vieira, M. Horie, H. Kato, M. Hoshino, F. Blanco, G. Garcia, S. J. Buckman, and H. Tanaka, J. Chem. Phys. **135**, 234309 (2011).
[16]M. Fuss, A. Muñoz, J. C. Oller, F. Blanco, D. Almeida, P. Limão-Vieira, T. P. D. Do, M. J. Brunger, and G. García, Phys. Rev. A **80**, 052709 (2009).
[17]L. Boesten, H. Tanaka, A. Kobayashi, M. A. Dillon, and M. Kimura, J. Phys. B **25**, 1607 (1992).
[18]H. Kato, K. Anzai, T. Isihara, M. Hoshino, F. Blanco, G. Garcia, P. Limão-Vieira, M. J. Brunger, and H. Tanaka, "A study of electron interactions with silicon tetrafluoride: elastic scattering and vibrational excitation cross sections," J. Phys. B (in press).
[19]W. Sun, M. A. Morrison, W. A. Isaacs, W. K. Trail, D. T. Alle, R. J. Gulley, M. J. Brennan, and S. J. Buckman, Phys. Rev. A **52**, 1229 (1995).
[20]J. C. Nickel, P. W. Zetner, G. Shen, and S. Trajmar, J. Phys. E **22**, 730 (1989).
[21]L. Boesten and H. Tanaka, At. Data Nucl. Data Tables **52**, 25 (1992).
[22]M. A. Khakoo and S. Trajmar, Phys. Rev. A **34**, 138 (1986).
[23]D. T. Alle, R. J. Gulley, S. J. Buckman, and M. J. Brunger, J. Phys. B **25**, 1533 (1992).
[24]L. Campbell, M. J. Brunger, A. M. Nolan, L. J. Kelly, A. B. Wedding, J. Harrison, P. J. O. Teubner, D. C. Cartwright, and B. McLaughlin, J. Phys. B **34**, 1185 (2001).
[25]D. G. Thompson, Proc. R. Soc. London, Ser. A **294**, 160 (1966).
[26]G. G. Raju, IEEE Trans. Dielectr. Electr. Insul. **16**, 1199 (2009).
[27]R. D. Cowan, *The Theory of Atomic Structure and Spectra* (University of California Press, London, 1981).
[28]M. E. Riley and D. G. Truhlar, J. Chem. Phys. **63**, 2182 (1975).
[29]X. Z. Zhang, J. F. Sun, and Y. F. Liu, J. Phys. B **25**, 1893 (1992).
[30]G. Staszewska, D. W. Schwenke, D. Thirumalai, and D. G. Truhlar, Phys. Rev. A **28**, 2740 (1983).
[31]F. Blanco and G. García, Phys. Lett. A **295**, 178 (2002).
[32]F. Blanco and G. García, Phys. Rev. A **67**, 022701 (2003).
[33]O. Zatsarinny, K. Bartschat, G. Garcia, F. Blanco, L. R. Hargreaves, D. B. Jones, R. Murrie, J. R. Brunton, M. J. Brunger, M. Hoshino, and S. J. Buckman, Phys. Rev. A **83**, 042702 (2011).
[34]J. B. Maljković, A. R. Milosavljević, F. Blanco, D. Šević, G. García, and B. P. Marinković, Phys. Rev. A **79**, 052706 (2009).
[35]F. Blanco and G. Garcia, Phys. Lett. A **330**, 230 (2004).
[36]F. Blanco and G. García, J. Phys. B **42**, 145203 (2009).
[37]T. Sakae, S. Sumiyoshi, E. Murakami, Y. Matsumoto, K. Ishibashi, and A. Katase, J. Phys. B **22**, 1385 (1989).
[38]See http://www.wiredchemist.com/chemistry/data/bond-energies-lengths for tabulated values of the relevant bond lengths of the species in question.